


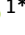



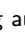



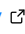

1 GIRFReco.jl: An Open-Source Pipeline for Spiral 2 Magnetic Resonance Image (MRI) Reconstruction in 3 Julia

4 Alexander Jaffray ^{1,2*} , Zhe Wu ^{1*} , S. Johanna Vannesjo ³, Kâmil
5 Uludağ ^{1,4}, and Lars Kasper ¹

6 **1** Krembil Research Institute, University Health Network, Ontario, Canada **2** MRI Research Centre,
7 University of British Columbia, Vancouver, Canada **3** Department of Physics, Norwegian University of
8 Science and Technology, Trondheim, Norway **4** Department of Medical Biophysics, University of Toronto,
9 Canada  Corresponding author * These authors contributed equally.

DOI: [10.xxxxxx/draft](https://doi.org/10.xxxxxx/draft)

Software

- [Review](#) 
- [Repository](#) 
- [Archive](#) 

Editor: [Kevin M. Moerman](#) 

Reviewers:

- [@cncastillo](#)
- [@mathieboudreau](#)
- [@felixhorger](#)

Submitted: 01 June 2023

Published: unpublished

License

Authors of papers retain copyright
and release the work under a
Creative Commons Attribution 4.0
International License ([CC BY 4.0](#)).

10 Summary

11 Magnetic Resonance Imaging (MRI) acquires data in the frequency domain (k-space), with
12 ~~the sampling pattern~~ traversed by a path known as the k-space trajectory. It is desirable
13 to implement MRI data sampling using k-space trajectories with high acquisition efficiency
14 (i.e., a fast coverage of k-space). Traditional Cartesian MRI traverses k-space by acquiring
15 individual lines of the k-space, each requiring an excitation, a phase-encoding step, and a
16 ~~short~~ readout gradient. However, it is possible to traverse k-space with an arbitrary trajectory,
17 achieved by a long sequence of readout gradients, thus presenting the opportunity to acquire
18 more sampling points per excitation. Spiral trajectories are a popular and efficient method
19 for traversing k-space with a long ~~readout~~, as well as classical echo-planar imaging (EPI)
20 trajectories. Non-Cartesian trajectories, such as spiral trajectories, yield significant reductions
21 in the number of excitations required for the acquisition of an image, thus offering considerable
22 acceleration and improvements in signal-to-noise ratio (SNR) per unit time at the cost of
23 reconstruction complexity. These improvements are particularly beneficial in diffusion MRI due
24 to sequence timing constraints (Lee et al., 2021).

25 The actual k-space trajectory applied during the MRI experiment can differ from the nominal
26 trajectory due to hardware imperfections, resulting in image artifacts such as ghosting, blurring
27 or geometric distortion. This problem is exacerbated in many non-Cartesian trajectories, such
28 as spirals, because these fast imaging protocols place high demands on the gradient hardware
29 of the MRI system (Block & Frahm, 2005). Accurate characterization of the system hardware
30 is necessary and can be used for k-space trajectory correction, for example via a gradient
31 impulse response function (GIRF) (Addy et al., 2012; Vannesjo et al., 2013).

32 The high acquisition efficiency of non-Cartesian trajectories originates, in part, from the
33 prolonged readout duration which allows for more samples to be acquired per excitation
34 (single-shot or few-interleave scanning). However, when using such long readouts, the image
35 encoding scheme is susceptible to static off-resonance (or field inhomogeneity, B_0), resulting
36 in image artifacts ~~that scale with readout duration~~. For non-Cartesian trajectories, these
37 artifacts are difficult to correct in post-processing, but can be effectively addressed during
38 image reconstruction by incorporating spatial off-resonance measurements into the signal model
39 (Sutton et al., 2003).

40 Therefore, recent spiral imaging approaches often rely on an expanded signal model incorporating
41 system imperfections and off-resonance maps (Engel et al., 2018; Graedel et al., 2021; Kasper
42 et al., 2018; Kasper et al., 2022; Lee et al., 2021; Robison et al., 2019; Vannesjo et al., 2016;

43 [Wilm et al., 2011, 2015](#)), in combination with parallel imaging acceleration using multiple
44 receiver coils and iterative non-Cartesian image reconstruction algorithms, e.g., CG-SENSE
45 ([Pruessmann et al., 2001](#)).

46 Here, we introduce the open-source GIRFReco.jl reconstruction pipeline, which provides a
47 single ecosystem implementation of this state-of-the-art approach to non-Cartesian MRI in the
48 programming language Julia ([Bezanson et al., 2017](#)). The core reconstruction routines rely
49 upon the public Julia package MRIReco.jl, a comprehensive open-source image reconstruction
50 toolbox. To enable robust, accessible and fast MRI with spiral gradient waveforms, GIRFReco.jl
51 is designed as an end-to-end signal processing pipeline, from open-standard raw MR data
52 ([ISMR]MRD ([Inati et al., 2017](#))) to final reconstructed images (NIFTI neuroimage data format
53 (NIFTI, 2003)). It integrates system characterization information via GIRF correction for
54 accurate representation of the encoding fields, relevant calibration data (coil sensitivity and
55 static off-resonance maps) and iterative parallel imaging reconstruction for non-Cartesian
56 k-space sampling patterns, including spiral trajectories.

57 Statement of Need

58 Existing open-source solutions for the correction of system imperfections and static off-resonance
59 in MRI are often implemented within the framework of mature image reconstruction suites
60 such as BART ([Blumenthal et al., 2022](#)), Gadgetron ([Hansen & Sørensen, 2013](#)) and MIRT
61 ([Fessler, n.d.](#)).

62 However, the aforementioned complexity of the image reconstruction task for spiral MRI
63 currently necessitates the integration of tools from multiple of these software suites in order to
64 establish a performant and comprehensive image reconstruction workflow (e.g., ([Veldmann et
65 al., 2022](#))). With each tool being developed in different programming languages (C for BART;
66 C++ for Gadgetron; MATLAB, C++ and C for MIRT, etc.), maintaining and extending such
an image reconstruction pipeline then requires cross-language expertise, adding significant
69 overhead and complexity to development. This presents a significant barrier to efficient and
70 reproducible image reconstruction and limits software accessibility and sustainability, especially
for users without software engineering backgrounds.

71 The programming language Julia ([Bezanson et al., 2017](#)) provides a practical solution to this
72 multiple-language problem by using a high-level interface to low-level compiled code, i.e.,
73 enabling fast prototyping with limited resources in an academic setting, while delivering a
74 near-industrial-level efficiency of code execution, all within a single development environment.

75 In this work, we introduce GIRFReco.jl (initial version presented at the annual meeting
76 of ISMRM 2022 ([Jaffray et al., 2022b](#))), which implements an end-to-end, self-contained
77 processing and image reconstruction pipeline for spiral MR data completely in Julia. Based
78 on the established MRIReco.jl package, GIRFReco.jl incorporates model-based corrections
79 ([Sutton et al., 2003](#); [Vannesjo et al., 2016](#); [Wilm et al., 2011, 2015](#)) to achieve high-quality spiral
80 MRI reconstructions. Specifically, this reconstruction pipeline combines several major steps: (1)
81 ESPIRiT coil sensitivity map estimation ([Uecker et al., 2014](#)); (2) Robust off-resonance (B_0)
82 map estimation ([Funai et al., 2008](#); [Lin & Fessler, 2020](#)); (3) Computation of the applied non-
83 Cartesian k-space trajectory using GIRF correction ([Vannesjo et al., 2013, 2016](#)); (4) Iterative
84 non-Cartesian MRI reconstruction (CG-SENSE) with off-resonance correction ([Knopp et al.,
85 2009](#); [Pruessmann et al., 2001](#)). Considering software reusability and sustainability, (1) and (4)
86 of the abovementioned steps are handled by MRIReco.jl, a comprehensive modular open-source
87 image reconstruction toolbox in Julia. Step (2), the B_0 map estimation, was developed as
88 a Julia package MRIFieldmaps.jl by the original authors ([Lin & Fessler, 2020](#)) with our
89 contribution of implementing an alternative algorithm ([Funai et al., 2008](#)) in Julia. Finally,
90 we implemented step (3), the GIRF correction, in an original Julia package MRIGradients.jl
91 ([Jaffray et al., 2022b](#)), porting and refactoring the MATLAB code of the original authors
92 ([Vannesjo & Graedel, 2020](#)).

93 **Functionality**

94 **Required Inputs**

95 GIRFReco.jl requires raw MRI (k-space) data (in [ISMR]MRD format (Inati et al., 2017)) of
96 the following scans as input:

- 97 1. Multi-echo Gradient-echo spin-warp (Cartesian) scan
98 ▪ must include at least two echo times (e.g., 4.92 ms and 7.38 ms at 3T)
- 99 2. Spiral scan
100 ▪ single or multi-interleave



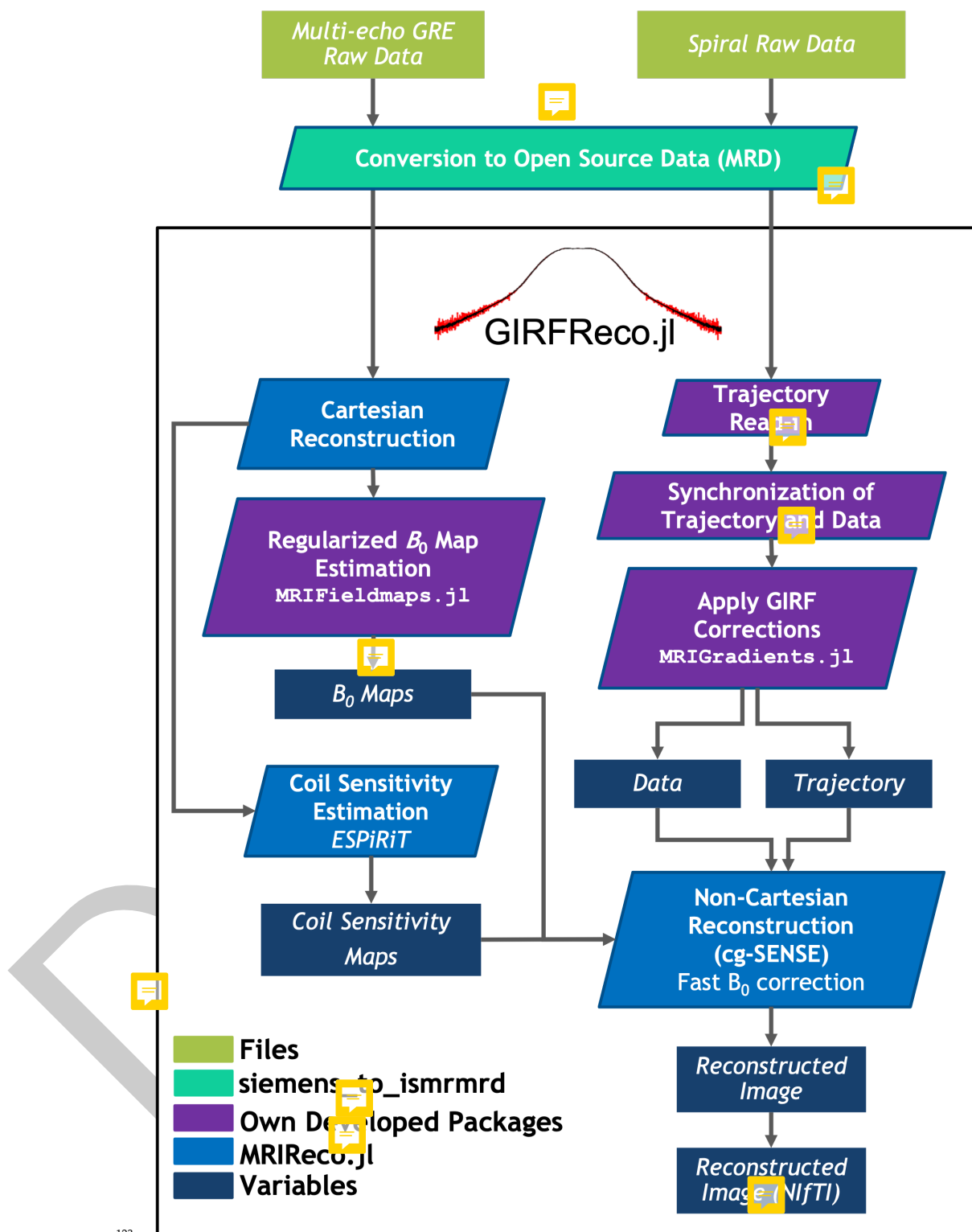
101 At the moment, the slice geometry (thickness, field-of-view, and direction) of the Cartesian and
102 spiral scans must be congruent, while the resolution does not need to be identical or isotropic.

103 **Overview of Components**

104 The following components are utilized within the spiral reconstruction pipeline of GIRFReco.jl
105 (Fig. 1), and called from their respective packages. We indicate where the authors of
106 GIRFReco.jl provided original contributions to the components by bold font.

- 107 1. Core iterative image reconstruction, using the Julia package MRIReco.jl
108 a. CG-SENSE (Pruessmann et al., 2001) algorithm for iterative non-Cartesian image
109 reconstruction
110 b. ESPIRiT (Uecker et al., 2014) for sensitivity map estimation
- 111 2. Model-based correction
112 a. Static off-resonance (B_0 inhomogeneity) correction
113 ▪ **Smoothed B_0 map estimation, using an implementation of (Funai et al.,**
114 **2008)** and MRIFieldMaps.jl (Lin & Fessler, 2020)
115 ▪ Static B_0 map correction, accelerated by a time-segmented implementation
116 (Knopp et al., 2009) in MRIReco.jl (Knopp & Grosser, 2021)
117 b. Encoding field (trajectory) correction via Gradient impulse response function (GIRF)
118 (Vannesjo et al., 2013)
119 ▪ Measurement with a phantom-based technique (Addy et al., 2012; Graedel et
120 al., 2017; Robison et al., 2019)
121 ▪ **Estimation using open-source code (Wu et al., 2022)**
122 ▪ **Prediction via MRIGradient.jl (Jaffray et al., 2022b)**





123
124 *Figure 1. Overview of the GIRFReco.jl signal processing and reconstruction pipeline. Depicted*
125 *is the workflow from raw acquired k-space data to the final reconstructed images with the*
126 *respective tasks (parallelogram), in/output data (rectangles) and the location of the processing*
127 *components within different packages (colours).*

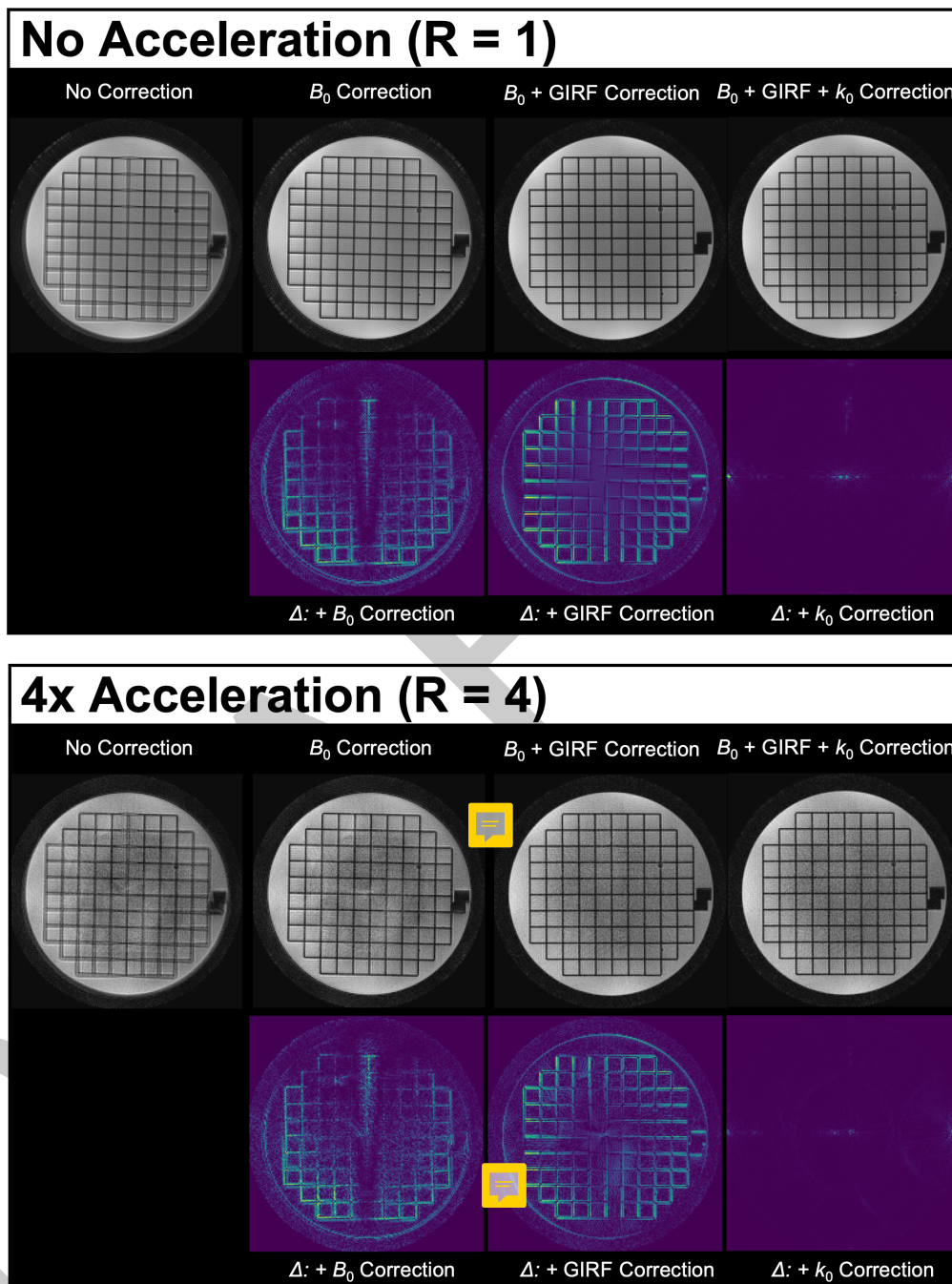
128 Detailed Processing Pipeline

129 GIRFReco.jl executes the steps required (depicted in Figure 1) for spiral diffusion reconstruction
130 in the following order:

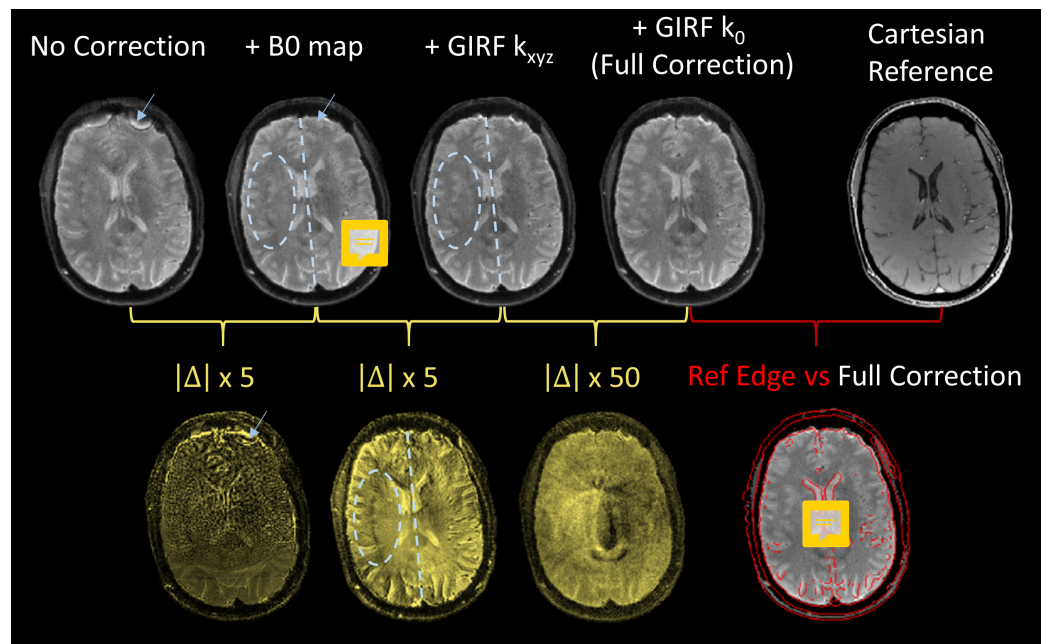
- 131 1. Conversion of proprietary, vendor-specific raw image data to an open-source raw data
132 format ([ISMR]MRD, (Inati et al., 2017)).
- 133 2. Reading of the trajectory or gradient sequence and synchronization of the k-space
134 trajectory onto the time course of the sampled k-space data to resolve any sampling rate
135 differences.
- 136 3. Model-based correction of the k-space sampling points (linear gradient self-terms) and
137 data (k_0 eddy currents) using the gradient impulse response function (GIRF (Vannesjo
138 et al., 2013), MRIGradients.jl (Jaffray et al., 2022b)).
- 139 4. Iterative reconstruction of Cartesian multi-echo gradient echo (GRE) scan.
- 140 5. Coil sensitivity map estimation (ESPIRiT (Uecker et al., 2014), MRIReco.jl) from the
141 first echo of multi-echo Cartesian GRE data.
- 142 6. Off-resonance (B_0) map estimation and processing (MRIFieldmaps.jl, (Funai et al.,
143 2008; Lin & Fessler, 2020)) based on multi-echo Cartesian GRE data.
- 144 7. Non-Cartesian, iterative parallel image reconstruction (cgSENSE) with off-resonance
145 correction ((Knopp et al., 2009; Pruessmann et al., 2001), MRIReco.jl (Knopp & Grosser,
146 2021)).

147 Via dedicated configuration files, individual steps can be selectively applied or skipped during
148 reconstruction, enabling assessment of the impact of different model-based corrections on
149 final image quality. We demonstrate this use case by providing example reconstructions
150 obtained from the GIRFReco.jl pipeline for a T_2 -weighted four-interleave spiral acquisition of
151 a geometric structure phantom by the American College of Radiology (ACR). Reconstructions
152 of both fully sampled and accelerated (using 1 of 4 interleaves, $R = 4$) datasets are depicted in
153 Figure 2. *In vivo* brain images reconstructed from a T_2 -weighted single-interleave ($R=4$) spiral
154 acquisition are presented in Figure 3 (Kasper et al., 2023). In all cases, improved image quality
155 was obtained by successively increasing the complexity of the applied model-based corrections
156 (nominal trajectory, added B_0 correction, GIRF-correction of gradients, GIRF correction of
157 k_0 eddy currents). The improvements in quality are best seen when looking at high-contrast
158 features of the images such as edges and corners, with subsequent corrections creating sharper
159 edge contrast and reducing blurring of small features.

160 Note that the reconstruction results from the phantom experiments (both $R = 1$ and $R = 4$
161 reconstructions in Figure 2) can be fully reproduced using GIRFReco.jl and the corresponding
162 dataset made publicly available (Jaffray et al., 2022a). For details, see the “Getting Started”
163 section below.



164
165 *Figure 2. Reconstructed four-interleave ($R=1$) and single-interleave ($R=4$) spiral images of a*
166 *selected slice of the ACR phantom. Top row, from left to right: Images reconstructed from the*
167 *nominal spiral gradient waveforms (“No Correction”), with correction for static off-resonance*
168 *(“ B_0 Correction”), $B_0 +$ GIRF correction of the k -space trajectory (“ $B_0 +$ GIRF Correction”),*
169 *and additional correction for GIRF k_0 eddy currents (“ $B_0 +$ GIRF + k_0 Correction”). Bottom*
170 *row: Stepwise difference images between subsequent corrections.*



171
172 *Figure 3. Reconstructed in-vivo spiral images of a human brain images (single interleave,*
173 *undersampling factor $R=4$). Top row: Images reconstructed from the nominal spiral gradient*
174 *waveform (“No correction”), with correction for static off-resonance (“ B_0 map”), B_0 + GIRF*
175 *correction of the k -space trajectory (“GIRF k_{xyz} ”), and additional correction for GIRF k_0*
176 *eddy currents (“Full Correction”). Bottom row: Consecutive absolute difference images of top-row*
177 *reconstructions (5x scaled, i.e., $\pm 20\%$ max image intensity; or 50x scaled, i.e., $\pm 2\%$*
178 *max image intensity). A Cartesian image (echo 1 from the B_0 map scan) is used as the*
179 *reference; its edges are overlaid to assess geometric congruency of the spiral images.*

180 Quality of Life Features

181 In addition to providing an end-to-end reconstruction workflow, GIRFReco.jl offers methods
182 for plotting images and calibration data at intermediate steps throughout the pipeline using
183 PlotlyJS. Furthermore, intermediate reconstruction results, such as calculated coil sensitivity
184 maps and B_0 maps are optionally stored as NIFTI files, a common neuroimaging data format
185 supported by various analysis and visualization packages (NIFTI, 2003).

186 Getting Started

187 Up-to-date information about how to install GIRFReco.jl, run example reconstructions (e.g.,
188 reproducing Figure 2) and apply it to your own data can be found in the README.md provided in
189 the GitHub repository. Further example scripts and technical documentation of GIRFReco.jl's
190 API, including its current feature set, is provided at <https://brain-to.github.io/GIRFReco.jl>,
191 automatically generated by Documenter.jl.

192 Conclusion and Outlook

193 The presented pipeline, GIRFReco.jl, is an open-source end-to-end solution for spiral MRI
194 reconstruction. It is developed in Julia, and allows users to obtain final images directly from
195 raw MR data acquired by spiral k -space trajectories. Following best practices of software
196 sustainability and accessibility, we rely on the established MR image reconstruction package
197 MRIReco.jl in our pipeline, while extending its capability to handle the more complex use
198 case of multiple model-based corrections, necessary for high-quality spiral MRI. Beyond spirals,

199 GIRFReco.jl can be readily utilized for data acquired under arbitrary non-Cartesian k-space
200 trajectories; its features of model-based MRI reconstruction with GIRF and off-resonance
201 corrections generalize to such sampling patterns in both 2D and 3D. Furthermore, GIRFReco.jl
202 can be extended to handle additional model-based corrections (e.g., concomitant or higher-order
203 encoding fields, (Bernstein et al., 1998; Vannesjo et al., 2016; Wilm et al., 2011, 2015)),
204 and act as a self-contained template for generalized image reconstruction from raw scan and
205 calibration data to interpretable and accessible images in Julia.

References

- 206
- 207 Addy, N. O., Wu, H. H., & Nishimura, D. G. (2012). Simple method for MR gradient system
208 characterization and k-space trajectory estimation. *Magnetic Resonance in Medicine*, *68*(1),
209 120–129. <https://doi.org/10.1002/mrm.23217>
- 210 Bernstein, M. A., Zhou, X. J., Polzin, J. A., King, K. F., Ganin, A., Pelc, N. J., & Glover, G. H.
211 (1998). Concomitant gradient terms in phase contrast MR: Analysis and correction. *Mag-*
212 *netic Resonance in Medicine*, *39*(2), 300–308. <https://doi.org/10.1002/mrm.1910390218>
- 213 Bezanson, J., Edelman, A., Karpinski, S., & Shah, V. B. (2017). Julia: A Fresh Approach to
214 Numerical Computing. *SIAM Review*, *59*(1), 65–98. <https://doi.org/10.1137/141000671>
- 215 Block, K. T., & Frahm, J. (2005). Spiral imaging: A critical appraisal. *Journal of Magnetic*
216 *Resonance Imaging*, *21*(6), 657–668. <https://doi.org/10.1002/jmri.20320>
- 217 Blumenthal, M., Holme, C., Roeloffs, V., Rosenzweig, S., Schaten, P., Scholand, N., Tamir,
218 J., Wang, X., & Uecker, M. (2022). *Mrirecon/bart: Version 0.8.00*. Zenodo. <https://doi.org/10.5281/ZENODO.592960>
- 219
- 220 Engel, M., Kasper, L., Barmet, C., Schmid, T., Vionnet, L., Wilm, B., & Pruessmann, K.
221 P. (2018). Single-shot spiral imaging at 7 T. *Magnetic Resonance in Medicine*, *80*(5),
222 1836–1846. <https://doi.org/10.1002/mrm.27176>
- 223 Fessler, J. A. (n.d.). *Michigan Image Reconstruction Toolbox*. Retrieved May 17, 2023, from
224 <https://github.com/JeffFessler/mirt>
- 225 Funai, A. K., Fessler, J. A., Yeo, D. T. B., Olafsson, V. T., & Noll, D. C. (2008). Regularized
226 Field Map Estimation in MRI. *IEEE Transactions on Medical Imaging*, *27*(10), 1484–1494.
227 <https://doi.org/10.1109/TMI.2008.923956>
- 228 Graedel, N. N., Hurley, S. A., Clare, S., Miller, K. L., Pruessmann, K. P., & Vannesjo, S. J.
229 (2017). *Comparison of gradient impulse response functions measured with a dynamic field*
230 *camera and a phantom-based technique*. 378.
- 231 Graedel, N. N., Kasper, L., Engel, M., Nussbaum, J., Wilm, B. J., Pruessmann, K. P.,
232 & Vannesjo, S. J. (2021). Feasibility of spiral fMRI based on an LTI gradient model.
233 *NeuroImage*, *245*, 118674. <https://doi.org/10.1016/j.neuroimage.2021.118674>
- 234 Hansen, M. S., & Sørensen, T. S. (2013). Gadgetron: An open source framework for medical
235 image reconstruction: Gadgetron. *Magnetic Resonance in Medicine*, *69*(6), 1768–1776.
236 <https://doi.org/10.1002/mrm.24389>
- 237 Inati, S. J., Naegele, J. D., Zwart, N. R., Roopchansingh, V., Lizak, M. J., Hansen, D.
238 C., Liu, C., Atkinson, D., Kellman, P., Kozerke, S., Xue, H., Campbell-Washburn, A.
239 E., Sørensen, T. S., & Hansen, M. S. (2017). ISMRM Raw data format: A proposed
240 standard for MRI raw datasets. *Magnetic Resonance in Medicine*, *77*(1), 411–421. <https://doi.org/10.1002/mrm.26089>
- 241
- 242 Jaffray, A., Wu, Z. (Tim), Uludağ, K., & Kasper, L. (2022a). *Data Supplement: Open-*
243 *source model-based reconstruction in Julia (ISMRM 2022)* [Data set]. Zenodo. <https://doi.org/10.5281/zenodo.6510021>
- 244

- 245 Jaffray, A., Wu, Z., Uludağ, K., & Kasper, L. (2022b). Open-source model-based reconstruction
246 in Julia: A pipeline for spiral diffusion imaging. *Proc. Intl. Soc. Mag. Reson. Med.* 30,
247 2435. <https://index.miramart.com/ISMRM2022/PDFfiles/2435.html>
- 248 Kasper, L., Engel, M., Barmet, C., Haeberlin, M., Wilm, B. J., Dietrich, B. E., Schmid, T.,
249 Gross, S., Brunner, D. O., Stephan, K. E., & Pruessmann, K. P. (2018). Rapid anatomical
250 brain imaging using spiral acquisition and an expanded signal model. *NeuroImage*, 168,
251 88–100. <https://doi.org/10.1016/j.neuroimage.2017.07.062>
- 252 Kasper, L., Engel, M., Heinzle, J., Mueller-Schrader, M., Graedel, N. N., Reber, J., Schmid,
253 T., Barmet, C., Wilm, B. J., Stephan, K. E., & Pruessmann, K. P. (2022). Advances in
254 spiral fMRI: A high-resolution study with single-shot acquisition. *NeuroImage*, 246, 118738.
255 <https://doi.org/10.1016/j.neuroimage.2021.118738>
- 256 Kasper, L., Wu, Z., Jaffray, A., Kashyap, S., & Uludağ, K. (2023). Feasibility of spiral diffusion
257 imaging on a clinical 3T MR system. *Proc. Intl. Soc. Mag. Reson. Med.* 31, 4164.
258 <https://index.miramart.com/ISMRM2023/PDFfiles/4164.html>
- 259 Knopp, T., Eggers, H., Dahnke, H., Prestin, J., & Senegas, J. (2009). Iterative Off-Resonance
260 and Signal Decay Estimation and Correction for Multi-Echo MRI. *IEEE Transactions on*
261 *Medical Imaging*, 28(3), 394–404. <https://doi.org/10.1109/TMI.2008.2006526>
- 262 Knopp, T., & Grosser, M. (2021). MRIReco.jl: An MRI reconstruction framework written in
263 Julia. *Magnetic Resonance in Medicine*, 86(3), 1633–1646. <https://doi.org/10.1002/mrm.28792>
264
- 265 Lee, Y., Wilm, B. J., Brunner, D. O., Gross, S., Schmid, T., Nagy, Z., & Pruessmann, K. P.
266 (2021). On the signal-to-noise ratio benefit of spiral acquisition in diffusion MRI. *Magnetic*
267 *Resonance in Medicine*, 85(4), 1924–1937. <https://doi.org/10.1002/mrm.28554>
- 268 Lin, C. Y., & Fessler, J. A. (2020). Efficient regularized field map estimation in 3D MRI. *IEEE*
269 *Transactions on Computational Imaging*, 6, 1451–1458. <https://doi.org/10.1109/TCI.2020.3031082>
270
- 271 NIFTI. (2003, September 2). *NIFTI Data Format* [National Institute of Mental Health Website].
272 Neuroimaging Informatics Technology Initiative. <https://nifti.nimh.nih.gov/>
- 273 Pruessmann, K. P., Weiger, M., Börner, P., & Boesiger, P. (2001). Advances in sensitivity
274 encoding with arbitrary k -space trajectories: SENSE With Arbitrary k -Space Trajectories.
275 *Magnetic Resonance in Medicine*, 46(4), 638–651. <https://doi.org/10.1002/mrm.1241>
- 276 Robison, R. K., Li, Z., Wang, D., Ooi, M. B., & Pipe, J. G. (2019). Correction of B_0
277 eddy current effects in spiral MRI. *Magnetic Resonance in Medicine*, 81(4), 2501–2513.
278 <https://doi.org/10.1002/mrm.27583>
- 279 Sutton, B. P., Noll, D. C., & Fessler, J. A. (2003). Fast, iterative image reconstruction for MRI
280 in the presence of field inhomogeneities. *IEEE Transactions on Medical Imaging*, 22(2),
281 178–188. <https://doi.org/10.1109/TMI.2002.808360>
- 282 Uecker, M., Lai, P., Murphy, M. J., Virtue, P., Elad, M., Pauly, J. M., Vasanawala, S.
283 S., & Lustig, M. (2014). ESPIRiT-an eigenvalue approach to autocalibrating parallel
284 MRI: Where SENSE meets GRAPPA. *Magnetic Resonance in Medicine*, 71(3), 990–1001.
285 <https://doi.org/10.1002/mrm.24751>
- 286 Vannesjo, S. J., & Graedel, N. N. (2020). *MRI-gradient / GIRF*. MRI-gradient. <https://github.com/MRI-gradient/GIRF>
287
- 288 Vannesjo, S. J., Graedel, N. N., Kasper, L., Gross, S., Busch, J., Haeberlin, M., Barmet, C.,
289 & Pruessmann, K. P. (2016). Image reconstruction using a gradient impulse response
290 model for trajectory prediction: GIRF-Based Image Reconstruction. *Magnetic Resonance*
291 *in Medicine*, 76(1), 45–58. <https://doi.org/10.1002/mrm.25841>

- 292 Vannesjo, S. J., Haeberlin, M., Kasper, L., Pavan, M., Wilm, B. J., Barmet, C., & Pruessmann,
293 K. P. (2013). Gradient system characterization by impulse response measurements with a
294 dynamic field camera: Gradient System Characterization with a Dynamic Field Camera.
295 *Magnetic Resonance in Medicine*, 69(2), 583–593. <https://doi.org/10.1002/mrm.24263>
- 296 Veldmann, M., Ehses, P., Chow, K., Nielsen, J., Zaitsev, M., & Stöcker, T. (2022). Open-source
297 MR imaging and reconstruction workflow. *Magnetic Resonance in Medicine*, 88(6),
298 2395–2407. <https://doi.org/10.1002/mrm.29384>
- 299 Wilm, B. J., Barmet, C., Pavan, M., & Pruessmann, K. P. (2011). Higher order reconstruction
300 for MRI in the presence of spatiotemporal field perturbations: Higher Order Reconstruction
301 for MRI. *Magnetic Resonance in Medicine*, 65(6), 1690–1701. <https://doi.org/10.1002/mrm.22767>
- 303 Wilm, B. J., Nagy, Z., Barmet, C., Vannesjo, S. J., Kasper, L., Haeberlin, M., Gross, S.,
304 Dietrich, B. E., Brunner, D. O., Schmid, T., & Pruessmann, K. P. (2015). Diffusion MRI
305 with concurrent magnetic field monitoring: Diffusion MRI with Concurrent Magnetic Field
306 Monitoring. *Magnetic Resonance in Medicine*, 74(4), 925–933. <https://doi.org/10.1002/mrm.25827>
- 308 Wu, Z., Jaffray, A., Vannesjo, S. J., Uludağ, K., & Kasper, L. (2022). MR System Stability and
309 Quality Control using Gradient Impulse Response Functions (GIRF). *Proc. Intl. Soc. Mag.
310 Reson. Med.* 30, 0641. <https://index.miramart.com/ISMRM2022/PDFfiles/0641.html>

DRAFT